Dissipative dynamics at first-order quantum transitions

Giovanni Di Meglio,[1] Davide Rossini,[2] and Ettore Vicari[2,*]
[1]*Dipartimento di Fisica dell'Università di Pisa, Largo Pontecorvo 3, I-56127 Pisa, Italy*
[2]*Dipartimento di Fisica dell'Università di Pisa and INFN, Largo Pontecorvo 3, I-56127 Pisa, Italy*

(Received 28 September 2020; revised 19 November 2020; accepted 20 November 2020; published 4 December 2020)

We investigate the effects of dissipation on the quantum dynamics of many-body systems at quantum transitions, especially considering those of the first order. This issue is studied within the paradigmatic one-dimensional quantum Ising model. We analyze the out-of-equilibrium dynamics arising from quenches of the Hamiltonian parameters and dissipative mechanisms modeled by a Lindblad master equation, with either local or global spin operators acting as dissipative operators. Analogously to what happens at continuous quantum transitions, we observe a regime where the system develops a nontrivial dynamic scaling behavior, which is realized when the dissipation parameter u (globally controlling the decay rate of the dissipation within the Lindblad framework) scales as the energy difference Δ of the lowest levels of the Hamiltonian, i.e., $u \sim \Delta$. However, unlike continuous quantum transitions where Δ is power-law suppressed, at first-order quantum transitions Δ is exponentially suppressed with increasing the system size (provided the boundary conditions do not favor any particular phase).

DOI: 10.1103/PhysRevB.102.224302

I. INTRODUCTION

The recent progress in atomic physics and quantum optical technologies has enabled great opportunities for a thorough investigation of the interplay between the coherent quantum dynamics and the (practically unavoidable) dissipative effects, due to the interaction with an external environment [1–4]. The competition between coherent and dissipative dynamic mechanisms may originate a nontrivial interplay, which can be responsible for the emergence of further interesting phenomena in many-body systems, in particular close to a quantum phase transition where the many-body systems develop peculiar quantum correlations [5].

Certain issues related to the competition between coherent and dissipative dynamics have been addressed at continuous quantum transitions (CQTs) [6–10], where quantum correlations develop diverging length scales ξ, and the gap Δ closes as a power law of ξ, i.e., $\Delta \sim \xi^{-z}$, z being the universal dynamic exponent. These studies considered a class of dissipative mechanisms which can be reliably described by a Lindblad master equation governing the time evolution of the system's density matrix. It was argued, and numerically checked, that a dynamic scaling limit exists at a CQT even in the presence of dissipation, whose main features are controlled by the universality class of the quantum transition. However, such a dynamic scaling limit requires a particular tuning of the dissipative interactions, whose decay rate u should scale as $u \sim \Delta \sim \xi^{-z}$.

In this paper we extend the above studies to first-order quantum transitions (FOQTs), which have their own peculiarities, in particular related to the emergence of an exponentially suppressed gap and to their sensitivity to the boundary conditions in finite systems [11–13]. Besides that, FOQTs are of great phenomenological interest, since they occur in a large variety of many-body systems, including quantum Hall samples [14], itinerant ferromagnets [15], heavy-fermion metals [16–18], disordered systems [19,20], and infinite-range models [21,22].

We address the interplay between the critical coherent dynamics and dissipative mechanisms, when the Hamiltonian parameters are close to a FOQT. To this purpose, we consider dynamic protocols that start from ground states close to FOQTs and then analyze the out-of-equilibrium dynamics arising from a instantaneous quench of the Hamiltonian parameters and the dissipative interaction with the environment. We take, as a paradigmatic example, the one-dimensional spin-1/2 quantum Ising model, exhibiting a FOQT line in its zero-temperature phase diagram, in the presence of either local or global homogeneous dissipative mechanisms—see Fig. 1. Their effects are assumed to be well captured by a Lindblad master equation of the density matrix of the open system. We mention that the dissipative dynamics of spin models at first-order transitions has been recently considered in Ref. [23], discussing various variants of the Lindblad equations.

Analogously to what happens at CQTs [8,9], the quantum Ising chain along the FOQT line unveils a regime where a nontrivial dynamic scaling behavior is developed. This is observed when the dissipation parameter u (globally controlling the decay rate of the dissipation within the master Lindblad equation) scales as the energy difference Δ of the lowest levels of the Hamiltonian of the many-body system, i.e., $u \sim \Delta$. However, unlike CQTs where Δ is power-law suppressed, at FOQTs Δ is exponentially suppressed with increasing the system size (when the boundary conditions do not favor any particular phase). The dynamic scaling behavior turns out to become apparent for relatively small systems already, such as chains with $L \lesssim 10$. This makes such dynamic scaling phenomena particularly interesting even from an experimental point of view, where the technical difficulties in manipulating

*Authors are listed in alphabetic order.

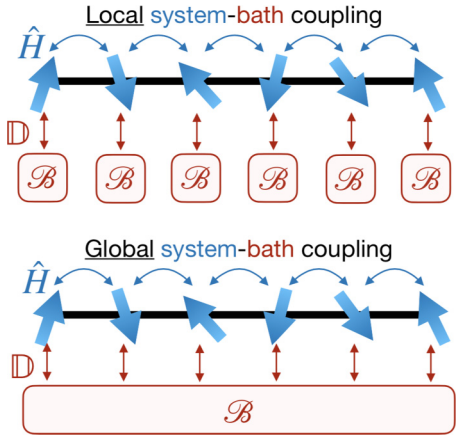

FIG. 1. The quantum spin-chain model discussed in this work. Neighboring spins are coupled through a coherent Hamiltonian $\hat{H}$ (bidirectional blue arrows). Each spin is also homogeneously and weakly coupled to some external bath $\mathcal{B}$ via a set of dissipators $\mathbb{D}$ (vertical red arrows), whose effect is to induce incoherent dissipation. The environment is modeled either as a sequence of local independent baths, each for any spin of the chain (top drawing), or as a single common bath to which each spin is supposed to be uniformly coupled (bottom drawing).

and controlling such systems can be probably faced with up-to-date methods. Here the out-of-equilibrium quantum dynamics associated with the above-mentioned protocol is numerically monitored by considering standard observables, such as the longitudinal magnetization, as well as the average work and heat characterizing the quantum thermodynamic properties of the out-of-equilibrium phenomenon.

The paper is organized as follows. In Sec. II we introduce the one-dimensional quantum Ising chain, the modelization of the dissipative interactions through a master Lindblad equation, and the out-of-equilibrium protocol discussed hereafter. Section III presents a summary of the main features of the dynamic scaling theory for closed systems and their extension to allow for dissipative interactions; in particular we address the behavior expected at FOQTs. In Sec. IV we numerically study the dynamics of quantum Ising chains arising from the above-mentioned protocol, up to the size of order $L = 10$, along the FOQTs and at the CQT, showing that the results support the general dynamic scaling theory. Finally in Sec. V we summarize and draw our conclusions. In Appendix A we solve the analogous problem for a single quantum spin. In Appendix B we address some related questions for the out-of-equilibrium behavior of the Kitaev fermionic wire (related to the quantum Ising chain by a Jordan-Wigner mapping) in the presence of local dissipation due to particle pumping or decay, at its CQT; these include exact analytic results for the quantum work and the heat interchange during its time evolution.

II. THE OUT-OF-EQUILIBRIUM PROTOCOL

The Hamiltonian of the one-dimensional ferromagnetic quantum Ising model reads:

$$\hat{H}(g,h) = -J \sum_{x=1}^{L} \left[\hat{\sigma}_x^{(1)} \hat{\sigma}_{x+1}^{(1)} + g\,\hat{\sigma}_x^{(3)} + h\,\hat{\sigma}_x^{(1)} \right], \qquad (1)$$

where $\hat{\sigma}_x^{(k)}$ are spin-1/2 Pauli matrices associated with the xth site of the chain, $J > 0$ sets the energy scale, and we assume a transverse field with strength $g \geqslant 0$. We also consider spin systems of size L with periodic boundary conditions.

It is well known that, at $g = g_c = 1$ and $h = 0$, the model undergoes a CQT separating a disordered phase ($g > 1$) from an ordered ($g < 1$) one [5]. The corresponding quantum critical behavior belongs to the two-dimensional Ising universality class, characterized by a diverging length scale ($\xi \sim |g - g_c|^{-\nu}$, with $\nu = 1$) and the power-law suppression of the gap Δ between the two lowest energy levels (as $\Delta \sim \xi^{-z}$ with $z = 1$, or as $\Delta \sim L^{-z}$ in finite-size systems at the critical point).

The FOQT line, located at $g < g_c = 1$, is related to the level crossing of the two lowest states $|\uparrow\rangle$ and $|\downarrow\rangle$ for $h = 0$, such that $\langle\uparrow|\hat{\sigma}_x^{(1)}|\uparrow\rangle = m_0$ and $\langle\downarrow|\hat{\sigma}_x^{(1)}|\downarrow\rangle = -m_0$ (independently of x), with $m_0 > 0$. The degeneracy of these states is lifted by the longitudinal field, with strength h. Therefore, $h = 0$ is a FOQT point, where the ground-state longitudinal magnetization

$$M = \langle \hat{\Sigma}^{(1)} \rangle\,, \quad \hat{\Sigma}^{(1)} \equiv \frac{1}{L} \sum_x \hat{\sigma}_x^{(1)}\,, \qquad (2)$$

becomes discontinuous in the infinite-volume limit. The transition separates two different phases characterized by opposite values of the magnetization m_0, i.e., [24]

$$\lim_{h\to 0^{\pm}} \lim_{L\to\infty} M = \pm m_0\,, \quad m_0 = (1-g^2)^{1/8}\,. \qquad (3)$$

In a finite system of size L with either periodic or open boundary conditions (which do not favor any of the two magnetized phases separated by the FOQT), the lowest states are superpositions of the two magnetized states $|\uparrow\rangle$ and $|\downarrow\rangle$. Due to tunneling effects, the energy gap at $h = 0$ vanishes exponentially as L increases [11,25], as $\Delta_L \sim e^{-cL^d}$. In particular, for the one-dimensional case of the model (1), the gap at $h = 0$ behaves as [24,26] $\Delta_L \approx 2\,(1-g^2)g^L$ for open boundary conditions and

$$\Delta_L \approx 2\sqrt{\frac{1-g^2}{\pi L}}\, g^L \qquad (4)$$

for periodic boundary conditions. The differences $E_i - E_0$ for the higher excited states ($i > 1$) are finite for $L \to \infty$.

We model the dissipative interaction with the environment by Lindblad master equations for the density matrix of the system [27,28],

$$\frac{\partial \rho}{\partial t} = -\frac{i}{\hbar}\,[\hat{H}, \rho] + u\,\mathbb{D}[\rho]\,, \qquad (5)$$

where the first term in the r.h.s. provides the coherent driving, while the second term accounts for the coupling to the environment. Its form depends on the nature of the dissipation arising from the interaction with the bath, which is effectively described by a set of dissipators $\mathbb{D}$ and a global coupling $u > 0$. In quantum optical implementations, the conditions leading to such a framework to study dissipative phenomena are typically satisfied [29], therefore this formalism constitutes a standard choice for theoretical investigations of such kind of systems.

In the following, we restrict to homogeneous dissipation mechanisms, preserving translational invariance. We mostly consider local dissipative mechanisms such as the one sketched in the top drawing of Fig. 1, whose trace-preserving superoperator $\mathbb{D}[\rho]$ can be written as [30,31]

$$\mathbb{D}[\rho] = \sum_{x=1}^{L} \hat{L}_x \rho \hat{L}_x^\dagger - \frac{1}{2}\left(\rho\, \hat{L}_x^\dagger \hat{L}_x + \hat{L}_x^\dagger \hat{L}_x \rho\right). \tag{6}$$

The Lindblad jump operator $\hat{L}_x$ associated to the local system-bath coupling scheme is chosen to be

$$\hat{L}_x^\pm \equiv \hat{\sigma}_x^\pm = \tfrac{1}{2}\left[\hat{\sigma}_x^{(1)} \pm i\hat{\sigma}_x^{(2)}\right], \tag{7}$$

corresponding to mechanisms of incoherent raising (+) or lowering (−) for each spin of the chain. We shall also consider an alternative global dissipative interaction with the environment (bottom drawing of Fig. 1), described by

$$\mathbb{D}[\rho] = \hat{L}\rho\hat{L}^\dagger - \tfrac{1}{2}(\rho\, \hat{L}^\dagger \hat{L} + \hat{L}^\dagger \hat{L}\rho), \tag{8}$$

with a single raising, or lowering, Lindblad operator

$$\hat{L}^\pm \equiv \hat{\Sigma}^\pm, \quad \hat{\Sigma}^\pm \equiv \frac{1}{L}\sum_x \hat{\sigma}_x^\pm. \tag{9}$$

In the following, we address the interplay between the coherent dynamics and dissipative mechanisms, focusing in particular on the cases $g \leqslant 1$ and $|h| \ll 1$, corresponding to situations close to the transition line. For this purpose, we consider dynamic protocols that start from ground states of the quantum Ising Hamiltonian close to the transition line and then analyze the out-of-equilibrium dynamics driven by the master Lindblad equation (5). More precisely, we adopt the following protocol: (i) the system starts, at $t = 0$, from the ground state of the Hamiltonian (1) with transverse field parameter $g \leqslant 1$ and the longitudinal parameter h_i; (ii) then the system evolves according to Eq. (5), where the coherent driving is provided by the Hamiltonian for the same value g and a longitudinal parameter h (which may differ from h_i, giving rise to a sudden quench), while the dissipative driving is controlled by the parameter u (for $u = 0$, one recovers the unitary dynamics of closed systems).

The out-of-equilibrium evolution, for $t > 0$, is monitored by measuring certain fixed-time observables, such as the longitudinal magnetization

$$M(t, h_i, h, L) = \mathrm{Tr}[\rho(t)\, \hat{\Sigma}^{(1)}], \tag{10}$$

where the spin operator $\hat{\Sigma}^{(1)}$ is defined in Eq. (2) and $\rho(t)$ is the density matrix of the evolving system at time t. Analogously, one may also consider fixed-time spin correlations.

We are also interested in the quantum thermodynamic properties associated with this dissipative dynamics. The first law of thermodynamics describing the energy flows of the global system, including the environment, can be written as [32–34]

$$\frac{dE_s}{dt} = w(t) + q(t), \tag{11}$$

where E_s is the average energy of the open system

$$E_s = \mathrm{Tr}\,[\rho(t)\hat{H}(t)], \tag{12}$$

and

$$w(t) \equiv \frac{dW}{dt} = \mathrm{Tr}\left[\rho(t)\,\frac{d\hat{H}(t)}{dt}\right], \tag{13}$$

$$q(t) \equiv \frac{dQ}{dt} = \mathrm{Tr}\left[\frac{d\rho(t)}{dt}\,\hat{H}(t)\right], \tag{14}$$

with W and Q, respectively, denoting the average work done on the system and the heat interchanged with the environment.

In our quench protocol, a nonvanishing work is only done at $t = 0$, when the longitudinal-field parameter suddenly changes from h_i to $h \neq h_i$. Since, after quenching the field, the Hamiltonian is kept fixed [thus $w(t) = 0$, for $t > 0$], the average work is simply given by the static expectation value

$$W = \langle 0_{h_i}|\hat{H}(h) - \hat{H}(h_i)|0_{h_i}\rangle = (h_i - h)L\,\langle 0_{h_i}|\hat{\Sigma}^{(1)}|0_{h_i}\rangle, \tag{15}$$

where $|0_{h_i}\rangle$ is the starting ground state associated with the longitudinal parameter h_i. Note that the average work of this protocol is the same as that arising at sudden quenches of closed Ising chains, whose scaling behavior at the CQT and FOQTs has been analyzed in Ref. [35]. On the other hand, the heat interchange with the environment is strictly related to the dissipative mechanism, indeed one can easily derive the relation

$$q(t) = u\,\mathrm{Tr}[\mathbb{D}[\rho]\,\hat{H}(t)], \tag{16}$$

by replacing the r.h.s. of the Lindblad equation (5) into the expression (14).

III. DYNAMIC SCALING AT QUANTUM TRANSITIONS

We now summarize the main features of the dynamic scaling framework that we will exploit to analyze the out-of-equilibrium quantum dynamics of closed and open many-body systems. The scaling hypothesis is based on the existence of a nontrivial large-size limit, keeping appropriate scaling variables fixed.

We focus on the quantum Ising chain (1) along its transition line, thus for $g \leqslant 1$ and $|h| \ll 1$, corresponding to FOQTs for $g < 1$ and CQT for $g = 1$. Then we discuss the scaling behaviors arising from a longitudinal external field h, i.e.,

$$\hat{H}_h = -h\sum_x \hat{\sigma}_x^{(1)}. \tag{17}$$

The corresponding scaling variable controlling the equilibrium properties of isolated many-body systems at both CQTs and FOQTs can be generally written as the ratio [11,36]

$$\kappa(h) = E_h/\Delta_L, \tag{18}$$

between the L-dependent energy variation E_h associated with the $\hat{H}_h$ term and the energy difference $\Delta_L \equiv E_1 - E_0$ of the lowest-energy states at the transition point $h = 0$. Nonzero temperatures could be taken into account as well, by adding a further scaling variable $\tau = T/\Delta_L$. Dynamic behaviors, exhibiting nontrivial time dependencies, also require a scaling variable associated with the time variable, which is generally given by

$$\theta = \Delta_L\, t. \tag{19}$$

The equilibrium and dynamic scaling limits are defined as the large-size limit, keeping the above scaling variables fixed. Within this framework, the differences between CQTs and FOQTs are basically related to the functional dependence of the above scaling variables on the size: Typically, power laws arise at CQTs, while exponential laws emerge at FOQTs.

Specializing Eq. (18) to the FOQTs of the quantum Ising chain, we obtain the scaling variable [11]

$$\kappa(h) = 2m_0 hL/\Delta_L\,, \tag{20}$$

since $2m_0 hL$ quantifies the energy associated with the corresponding longitudinal-field perturbation $\hat{H}_h$, and $\Delta_L \sim g^L$. For example, in the equilibrium finite-size scaling limit, the magnetization is expected to behave as [11] $M(h, L) = m_0\, \mathcal{M}(\kappa)$, where $\mathcal{M}$ is a suitable scaling function. We point out that the FOQT scenario based on the avoided crossing of two levels is not realized for any boundary condition [11,13]: In fact, in some cases the energy difference Δ_L of the lowest levels may even display a power-law dependence on L. However, the scaling variable $\kappa(h)$ obtained using the corresponding Δ_L turns out to be appropriate, as well [11]. In the rest of the paper we shall restrict our study to quantum Ising models with boundary conditions that do not favor any of the two magnetized phases, such as periodic or open boundary conditions, which generally lead to exponential finite-size scaling laws. Thus also the scaling variable θ related to the time dependence, cf. Eq. (19), is subject to an exponential rescaling.

The CQT at $g = 1$ and $h = 0$ is characterized by power laws, irrespective of the boundary conditions (see, e.g., Ref. [37]). The corresponding scaling variable turns out to be

$$\kappa(h) \propto L^{y_h} h\,, \tag{21}$$

where $y_h = 15/8$ is the renormalization-group dimension of the longitudinal field h [see, e.g., Ref. [36] for its derivation from the general expression given in Eq. (18)]. Moreover, the energy difference between the two-lowest states behaves as $\Delta_L \sim L^{-z}$ where $z = 1$.

For example, let us consider a quench of the longitudinal field of a closed quantum Ising chain at $t = 0$, from h_i (starting from the corresponding ground state) to $h \neq h_i$. At both the FOQTs and the CQT, we expect that the quantum coherent evolution of the longitudinal magnetization (10) develops the dynamic scaling behavior

$$M(t, h_i, h, L) \approx L^{-\zeta} F_m(\theta, \kappa_i, \kappa)\,, \tag{22}$$

where

$$\kappa_i \equiv \kappa(h_i)\,, \quad \kappa \equiv \kappa(h)\,, \tag{23}$$

the exponent $\zeta = 1/8$ at the CQT (related to the renormalization-group dimension of the longitudinal spin variable), while $\zeta = 0$ at the FOQTs, and F_M is an appropriate scaling function. The approach to such asymptotic behavior is generally characterized by power-law corrections [11,36,37].

As discussed in Refs. [8,9], at CQTs the dissipator $\mathbb{D}[\rho]$ typically drives the system to a noncritical steady state, even when the Hamiltonian parameters are close to those leading to a quantum transition. However, one may identify a regime where the dissipation is sufficiently small to compete with the coherent evolution driven by the critical Hamiltonian, leading to potentially novel dynamic behaviors. At such a low-dissipation regime, a dynamic scaling framework can be observed after appropriately rescaling the global dissipation parameter u, cf. Eq. (5). Indeed, the master Lindblad equation (5) at the CQTs of the coherent Hamiltonian driving develops a scaling behavior as well [8–10], with a further dependence on the dissipation scaling variable

$$\gamma \equiv u/\Delta_L\,, \tag{24}$$

thus $\gamma \sim uL^z$. Therefore, in the presence of dissipation the dynamic scaling behavior (22) after quenching h is expected to change into

$$M(t, h_i, h, u, L) \approx L^{-\zeta} F_m(\theta, \kappa_i, \kappa, \gamma)\,. \tag{25}$$

Our working hypothesis for the study of analogous issues at FOQTs is that the dynamic scaling behavior (25) applies as well, with the same definition (24) of the dissipation scaling variable γ. In the following we challenge this scenario by means of numerical computations. For convenience, we calculate the rescaled longitudinal magnetization, defined as

$$\widetilde{M}(t, h_i, h, u, L) = \frac{M(t, h_i, h, u, L)}{M(0, h_i, h, u, L)}\,, \tag{26}$$

which is expected to behave as

$$\widetilde{M}(t, h_i, h, u, L) \approx \widetilde{F}_m(\theta, \kappa_i, \kappa, \gamma)\,, \tag{27}$$

at both the CQT and FOQTs. We recall that, according to our protocol, the initial longitudinal magnetization at $t = 0$ corresponds to that of the equilibrium ground-state expectation value for h_i. Therefore it satisfies the asymptotic scaling behavior [11,37]

$$M(0, h_i, h, u, L) \equiv M(h_i, L) \approx L^{-\zeta} f_m(\kappa_i)\,, \tag{28}$$

with $\zeta = 1/8$ at the CQT, $\zeta = 0$ at the FOQTs, and f_M being a universal scaling function (apart from a multiplicative normalization and a normalization of the argument) which depends on the type of transition, being a CQT or a FOQT.

IV. NUMERICAL RESULTS

In this section we present numerical results for the quantum Ising chain subject to the protocol described in Sec. II, when the system is close to the FOQT line, i.e., for $g < 1$ and $|h| \ll 1$. We also report some results at the CQT, for $g = 1$ and $|h| \ll 1$, extending the study already reported in Ref. [8], which focussed on the Kitaev fermionic wire (see also Appendix B). The latter is somehow related to the quantum Ising chain, although they are not equivalent, in particular in the presence of local dissipation. In all our simulations we set $\hbar = 1$, and $J = 1$ as the energy scale.

Numerically solving the Lindblad master equation (5) for a system as the one in Eq. (1) generally requires a huge computational effort, due to the large number of states in the many-body Hilbert space $\mathcal{H}$, which increases exponentially with the system size (dim $\mathcal{H} = 2^L$). More precisely, the time evolution of the density matrix $\rho(t)$, which belongs to the space of the linear operators on $\mathcal{H}$, can be addressed by manipulating a Liouvillian superoperator of size $2^{2L}\times 2^{2L}$. This severely limits the accessible system size to $L \lesssim 10$ sites, unless the model is amenable to a direct solvability. A notable

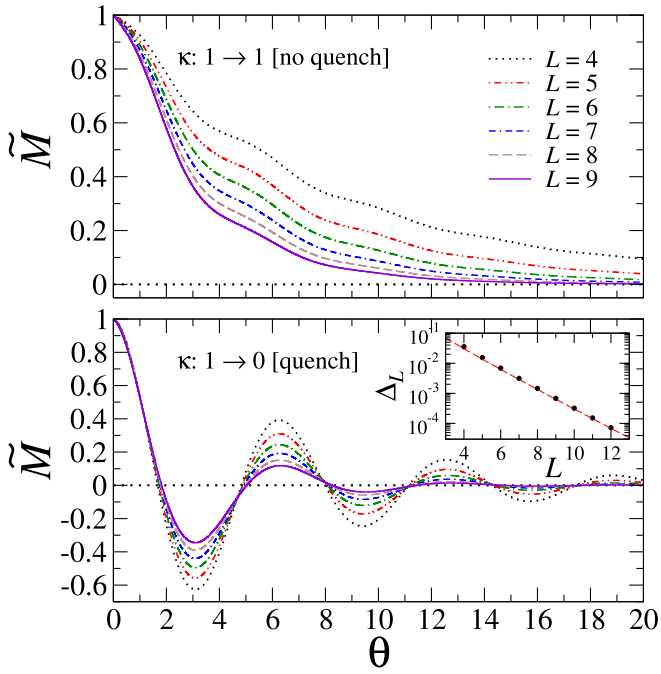

FIG. 2. Time behavior of the longitudinal magnetization for a quantum Ising ring close to the FOQT, with $g = 0.5$, in the presence of homogenous dissipation described by local Lindblad operators $\hat{L}_x^-$. We show the rescaled quantity $\widetilde{M}$ in Eq. (26) versus the rescaled time θ, for different values of the system size L (see legend). With increasing L, we keep the scaling variables $\kappa_i = 1$ and $\gamma = 0.1$ fixed. The upper panel is for $\kappa_i = \kappa$ (i.e., without the quench of the Hamiltonian parameter h), while the lower panel is for $\kappa = 0$. In the inset we show the energy gap Δ_L as a function of L: Black circles are the results obtained from the numerics, while the dashed red line denotes the estimate in Eq. (4).

example in this respect is the Kitaev chain with one-body Lindblad operators, whose corresponding Liouvillian operator is quadratic in the fermionic creation and annihilation operators (see, e.g., Ref. [8]). Unfortunately this is not the case for a dissipative Ising spin chain, in which the Jordan-Wigner mapping of Lindblad operators as those in (7) and (9) produces a nonlocal string operator forbidding an analytic treatment. Therefore, in this work we resort to a brute-force numerical integration of Eq. (5) through a fourth-order Runge-Kutta method, with a time step $dt = 10^{-2}$, sufficiently small to ensure convergence for all our purposes.

A. Dynamics along the FOQT line

In the following, we numerically challenge the dynamic scaling behavior put forward in Sec. III at the FOQTs. We provide results for quantum Ising chains with $g = 0.5$, up to lattice sizes $L = O(10)$. Computations for other values of $g < 1$ produce analogous results and are not explicitly shown here. Let us recall that our dynamic protocol starts from the ground state of the Hamiltonian (1) with longitudinal-field parameter h_i; then the system evolves according to the Lindblad master equation (5), with Hamiltonian parameter h (in principle different from h_i) and dissipative strength u.

Figure 2 displays the time evolution of the longitudinal magnetization (10), in particular the rescaled one defined in Eq. (26), for some selected values of dynamic scaling variables. The system-bath coupling has been modeled through local dissipative mechanisms as in the top drawing of Fig. 1, where the Lindblad operator associated to each site induces incoherent lowering of the corresponding spin ($\hat{L}_x^- = \hat{\sigma}_x^-$). The scaling behavior (27) is checked by varying the Hamiltonian and the dissipation parameters of the protocol with increasing size L, so that the scaling variables κ, κ_i, and γ [as defined in Eqs. (20), (23), and (24)] are kept fixed. For the gap Δ_L, entering the definition of the scaling variables $\theta = \Delta_L t$ and $\gamma = u/\Delta_L$, we do not use its asymptotic behavior (4), but the actual energy difference of the lowest levels of the quantum Ising ring at $h = 0$, with L spins (it passes from $\Delta_L \approx 3.55\times10^{-2}$ for $L = 4$, to $\Delta_L \approx 3.21\times10^{-4}$ for $L = 10$, as visible from the inset in the lower panel). In both cases considered in Fig. 2, namely for $\kappa_i = \kappa$ (top panel, without quenching the Hamiltonian) and for $\kappa_i \neq \kappa$ (bottom panel, in the presence of a Hamiltonian quench), the longitudinal magnetization appears to asymptotically vanish in the large-time limit, although with different qualitative trends. Actually this turns out to be a general feature for any nonzero value of the dissipation variable γ. Analogous results are obtained using Lindblad operators inducing incoherent raising of the corresponding spin ($\hat{L}_x^+ = \hat{\sigma}_x^+$).

Although limited to small system sizes, $L \leqslant 10$, our numerical results substantially support the dynamic scaling behavior conjectured in Eq. (27), especially for sufficiently small values of θ. Most likely, the large-L convergence is not uniform and tends to be slower with increasing θ. In particular, the results reported in the lower panel of Fig. 2 (when the dynamics arises both from a quench of the Hamiltonian parameter and from the presence of dissipation) display oscillations whose zeros nicely scale with the time scaling variable θ, even for quite large θ. On the other hand, the values at the maxima and minima undergo larger corrections, likely requiring larger lattice sizes to clearly observe the asymptotic scaling behavior. The apparent asymptotic convergence to the conjectured dynamic scaling is also suggested by the various plots in Fig. 3, showing data at fixed $\theta = 1$, for various values of κ and γ (panels on the left correspond to the two situations in Fig. 2, while panels on the right are for the analogous cases with a larger dissipation strength $\gamma = 0.5$). The approach to the large-L limit is generally compatible with $1/L$ corrections, as hinted by the dashed red lines, denoting $1/L$ fits of numerical data extrapolated at the largest available sizes.

B. Comparison with the single-spin problem

In the absence of dissipation, the dynamic scaling behavior of a quantum Ising chain along the FOQT turns out to be well described by an effective two-level problem [10,11,35,38], defined by the single-spin Hamiltonian

$$\hat{H}_s = a_1\,\hat{\sigma}^{(1)} + a_3\,\hat{\sigma}^{(3)}. \tag{29}$$

Indeed the dynamic scaling functions of the quantum Ising chain, when the boundary conditions do not favor any phase separated by the FOQT, match the dynamics of the single-spin

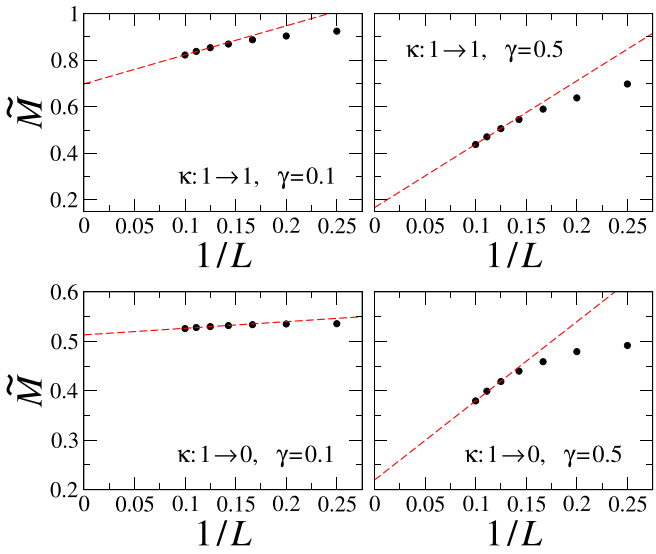

FIG. 3. Approach to the asymptotic dynamic scaling behavior of the longitudinal magnetization at the FOQT, in the presence of dissipation $\hat{L}_x^-$. Here we set $g = 0.5$, $\kappa_i = 1$, and $\theta = 1$, and show results for $\kappa = 0, 1$ and $\gamma = 0.1, 0.5$ (see indications in the panels). The data are roughly compatible with a global $1/L$ approach to the asymptotic dynamic scaling, in particular for $\gamma = 0.1$ (the dashed red lines are drawn to guide the eye).

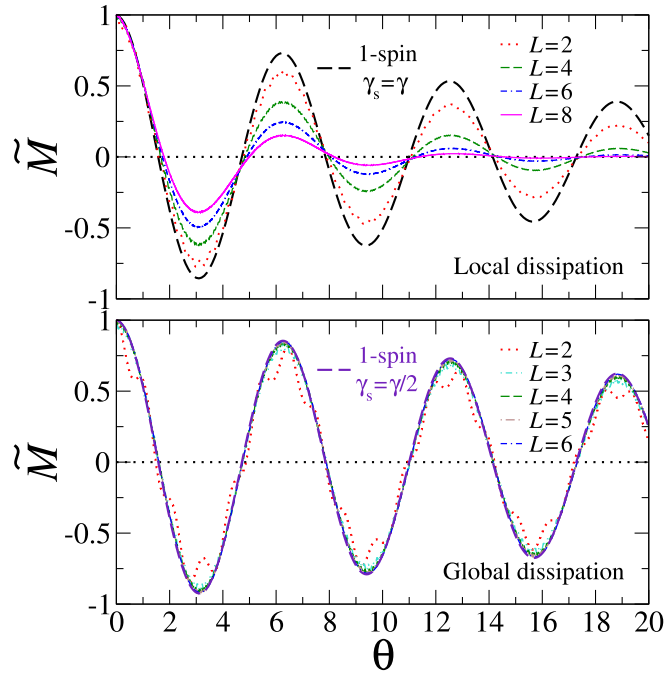

FIG. 4. Time behavior of the longitudinal magnetization at $g = 0.5$, in quench protocols with $\kappa_i = 100$, $\kappa = 0$, and $\gamma = 0.1$, for various values of L (see legends). The system bath coupling is implemented in the form of either local dissipation operators (6), with $\hat{L}_x = \hat{\sigma}_x^-$ (top panel), or a single global dissipation operator (8), with $\hat{L} = \Sigma^-$ (bottom panel). The numerical results are compared with the single-spin problem (thick-dashed curves): In the upper case, with increasing L, the curves tend to depart from the single-spin behavior; in the lower case, the curves appear to approach an asymptotic dynamic scaling behavior, which is well approximated by the solution of the single-spin problem with renormalized dissipation coupling $\gamma_s = \gamma/2 = 0.05$. In both cases, the frequencies of oscillations reasonably match.

problem (see Appendix A for an analytic discussion of the single-spin problem). In a sense, closed systems behave rigidly at FOQTs. We now want to understand whether that kind of property persists in the presence of dissipative interaction with an environment, such as in the two schemes sketched in Fig. 1.

In the presence of local dissipation (top drawing in Fig. 1), we observe that the asymptotic scaling behavior does not apparently display the rigidity property mentioned above, in that the scaling functions are not reproduced by the single-spin model. The corresponding data for the magnetization as a function of time are shown in the top panel of Fig. 4. The initial oscillating behavior at finite lengths is reasonably captured by the single-spin prediction with dissipation coupling $\gamma_s = \gamma$ [thick-dashed black line—see Eqs. (A17), (A21)]. However, already for $\theta \gtrsim 2$, the curves for $\tilde{M}$ exhibit large finite-size corrections and seem to approach an asymptotic overdamped behavior for $L \to \infty$, quickly reaching the zero value. In any case, the frequencies of oscillations for finite L values match those of the single-spin model, even for large θ.

The rigidity of the dynamic scaling behavior can be recovered if a global dissipative mechanism is considered (bottom drawing in Fig. 1). This is the case of the data reported in the bottom panel of Fig. 4. The curves for different L appear to approach an asymptotic dynamic scaling behavior, as well. Such convergence is much faster than that observed for the local dissipation scheme. Interestingly, the $L \to \infty$ behavior turns out to be well approximated by the solution of the single-spin problem (at least for $\theta \lesssim 5$), provided the dissipation coupling is suitably renormalized according to $\gamma_s = \gamma/2$ (thick-dashed violet line). We point out that this is a nontrivial result, since we are matching the full many-body dynamics close to a FOQT with a much simpler single-body behavior, by only admitting a nonuniversal renormalization of the various scaling variables.

C. Quantum work and heat

We now discuss the quantum thermodynamics arising from the out-of-equilibrium protocol. As already mentioned in Sec. II, a nonzero average work is only required at $t = 0$, when the Hamiltonian parameter suddenly changes from h_i to h. Therefore, it is the same as that of systems subject to quench protocols without dissipation (i.e., for $u = 0$). The dynamic scaling behavior of the work fluctuations for analogous quenches at the FOQTs of the quantum Ising chain was studied in Ref. [35], showing that they reproduce the analogous quantities of the single-spin problem. In particular, the average work is given by

$$W \approx \Delta_L \mathcal{W}(\kappa_i, \kappa), \quad \mathcal{W} = \frac{(\kappa_i - \kappa)\kappa_i}{2\sqrt{1+\kappa_i^2}}. \tag{30}$$

Reference [35] also reports results for the higher moments of work fluctuations and a discussion of the correction to the asymptotic behavior.

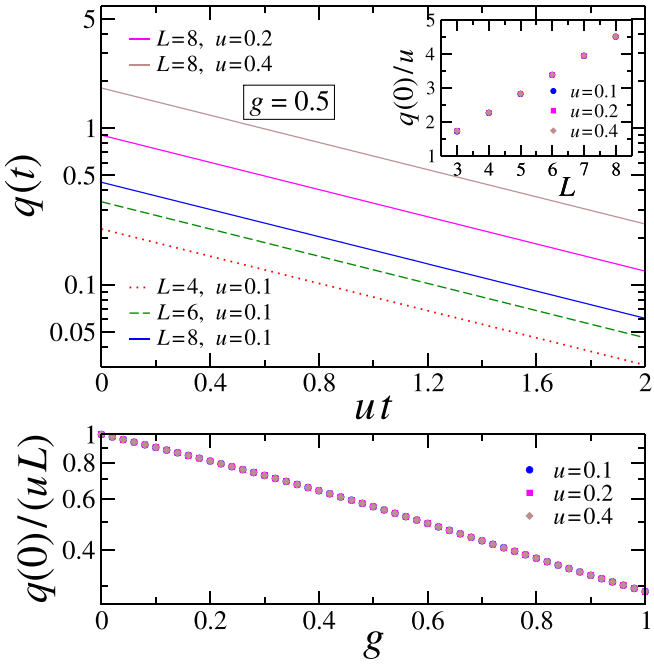

FIG. 5. Behavior of the heat interchanged between the quantum Ising chain and the environment, per unit of time, as a function of the variables of the system. Top panel: the function $q(t)$ with respect to the rescaled time ut, for different values of the system size L and of the dissipation strength u (see legend). In the inset we show the behavior of $q(t=0)/u$ with L, for various values of u. The transverse field strength is kept fixed at $g = 0.5$. Bottom panel: the function $q(t=0)/(uL)$ with respect to g, for $L = 6$ and various values of u. All the data reported in this figure as for $\kappa_i = \kappa = 0$, while the system-bath coupling is taken in the form of local and uniform Lindblad operators $\hat{L}_x^- = \hat{\sigma}_x^-$.

Coming to the heat interchanged between the system and the environment, for the sake of convenience here we focus on its time derivative $q(t) = dQ/dt$, defined in Eq. (14). Unlike for the average work, this quantity does not present any relevant scaling property. In particular, our numerical results for the dynamics of the quantum Ising chain homogeneously coupled to local incoherent lowering operators, cf. Eq. (6) with $\hat{L}_x^- = \hat{\sigma}_x^-$, clearly indicate an exponential decay of $q(t)$ with time t, as shown in the top panel of Fig. 5. More specifically, we found the following functional dependence on the various parameters of the system:

$$q(t) = C(g, \kappa_i, \kappa)\, u L\, e^{-ut}\,. \tag{31}$$

The coefficient $C(g, \kappa_i, \kappa)$ depends nearly exponentially on the transverse field g, although minor quantitative deviations are present (bottom panel). On the other hand, the dependence of C on both κ_i and κ is very weak and tends to vanish for increasing L (on the scale of the figure, it becomes unappreciable already for $L \gtrsim 8$).

Finally, it is worth emphasizing that the linear dependence of the rate of exchanged heat $q(t)$ with the system volume ($q \propto L$, as indicated in the top inset of Fig. 5) hints at the fact that such quantity is essentially related to a one-body mechanism, and not to a collective behavior of the system. In fact, the exponential time dependence $q(t) \sim e^{-ut}$ is identical to the single-spin model behavior, as emerging from the analysis in Appendix A [see, e.g., Eq. (A22)].

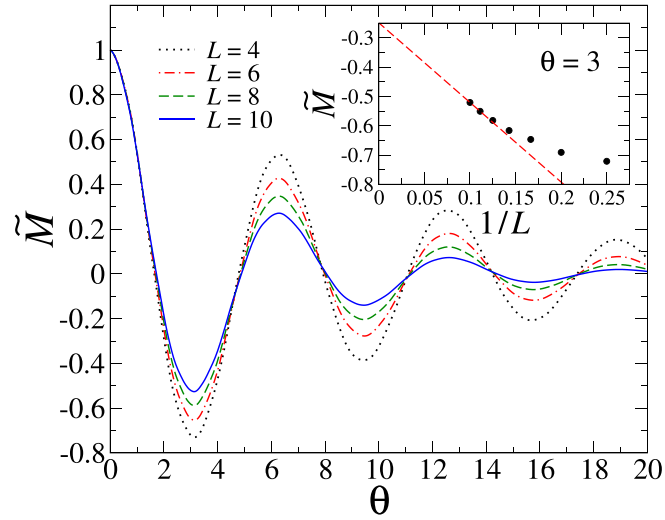

FIG. 6. Time behavior of the longitudinal magnetization for a quantum Ising chain at the CQT, in the presence of homogenous dissipation described by local Lindblad operators $\hat{L}_x^-$. We show the rescaled magnetization $\widetilde{M}$, cf. Eq. (26), versus the rescaled time θ, for different values of the system size L (see legend). With increasing L we keep the scaling variables $\kappa_i = 1$, $\kappa = 0$ and $\gamma = 0.1$ fixed. The inset displays data at fixed $\theta = 3$ versus $1/L$, showing that they are roughly compatible with a $1/L$ approach to the asymptotic dynamic scaling (the dashed red line is drawn to guide the eye), although further corrections are clearly visible.

D. Dynamics at the CQT

We now discuss the dynamic scaling behavior at the CQT (i.e., at $g = 1$ and $|h| \ll 1$), focusing on the longitudinal magnetization [see Eq. (27)]. Figure 6 reports the rescaled quantity $\widetilde{M}$ versus the rescaled time $\theta = tL^{-z}$, for various systems sizes, up to $L = 10$. The curves with increasing L are obtained keeping the scaling variables $\kappa_i \sim h_i L^{y_h}$, $\kappa \sim h L^{y_h}$, and $\gamma \sim u L^z$ (with $y_h = 15/8$ and $z = 1$) fixed. The displayed data are for $\kappa_i = 1$, $\kappa = 0$, $\gamma = 0.1$, but analogous qualitative conclusions can be drawn by changing the specific values of such rescaled quantities. Our results substantially support the dynamic scaling behavior conjectured in Eq. (27), in particular for sufficiently small values of θ. The approach to the asymptotic behavior is again compatible with $1/L$ corrections, as expected (see the inset, where numerical data for the rescaled magnetization at fixed $\theta = 3$ are plotted against the inverse system size, and the dashed red line denotes a $1/L$ fit of such data at large L). We point out that analogous dynamic scaling behaviors have been reported for the Kitaev fermionic wire (see Appendix B), where much larger sizes can be reached, allowing us to achieve a definitely more robust check of the dynamic scaling behavior at a CQT [8,9].

Again the quantum thermodynamics arising from the dynamic protocol is characterized by an initial work at $t = 0$, due to the quench of the Hamiltonian parameter. Its scaling behavior was already discussed in Ref. [35] for closed systems. As demonstrated there, the average work shows the scaling

behavior

$$W \approx L^{-z}\,\mathcal{W}(\kappa_i, \kappa)\,. \tag{32}$$

In Appendix B we discuss the average work within the Kitaev fermionic wire at its CQT, where the quench is performed over the chemical potential, corresponding to the transverse field g of the Ising chain. As shown there, the leading contribution to the average work is provided by analytical terms, while the scaling part, such as that in Eq. (32), turns out to be subleading.

On the other hand, even at the CQT, the heat interchanged with the environment does not exhibit scaling properties. We have observed an exponential decay in time and a trivial linear dependence with L, for the function $q(t)$, analogously as in Eq. (31). The only difference with respect to the $g < 1$ case is an enhanced sensitivity of the coefficient $C(g = 1, \kappa_i, \kappa)$ on the rescaled longitudinal field parameters, κ_i and κ, which however rapidly reduces with increasing L.

V. CONCLUSIONS

We have investigated the effects of dissipation on the quantum dynamics of many-body systems close to a FOQT (that is, whose Hamiltonian parameters are those leading to a FOQT for the closed system), arising from the interaction with the environment, as for example sketched in Fig. 1. The latter is modeled through a class of dissipative mechanisms that can be effectively described by Lindblad equations (5) for the density matrix of the system [27,28], with local or global homogenous Lindblad operators, such as those reported in Eqs. (6)-(7) or (8)-(9), respectively. This framework is of experimental interest, indeed the conditions for its validity are typically realized in quantum optical implementations [29]. We have analyzed how homogenous dissipative mechanisms change the dynamic scaling laws developed by closed systems at FOQTs (see, e.g., Refs. [13,38]). We also mention that analogous issues have been addressed at CQTs (see, e.g., Refs. [8–10]).

We study the above issues within the paradigmatic one-dimensional quantum Ising model, cf. Eq. (1), which provides an optimal theoretical laboratory for the investigation of phenomena emerging at quantum transitions. Indeed its zero-temperature phase diagram presents a line of FOQTs driven by a longitudinal external field, ending at a continuous quantum transition. To investigate the interplay between coherent and dissipative drivings at the quantum-transition line (FOQTs for $g < 1$ and $|h| \ll 1$ and CQT for $g \approx 1$ and $|h| \ll 1$), we consider the following dynamic protocol. The system is initialized, at $t = 0$, into the ground state of the Hamiltonian (1), for a given longitudinal parameter h_i; then, for $t > 0$, it evolves according to the Lindblad equation (5), where the coherent driving is provided by $\hat{H}(g, h)$, with h generally different from h_i, and the system-bath interaction effectively described by the dissipator $\mathbb{D}[\rho]$ with a fixed coupling strength u.

Analogously to what happens at CQTs, we observe a regime where the system develops a nontrivial dynamic scaling behavior, which is realized when the dissipation parameter u scales as the energy difference Δ of the lowest levels of the Hamiltonian of the many-body system. However, unlike CQTs where Δ is power-law suppressed, at FOQTs Δ is exponentially suppressed when boundary conditions do not favor any particular phase [11,13]. Numerical solutions of the Lindblad equations up to lattice sizes with $L \approx 10$ substantially confirm the existence of such dynamic scaling behavior and pave the way toward experimental testing in the near future through quantum simulation platforms for spin systems of small size, where the required resources are less demanding.

We also compare the emerging asymptotic scaling behavior with the single-spin problem interacting with an environment modeled by a corresponding Lindblad equation. Unlike closed systems where the unitary dynamics is well described by the two-level single-spin problem, in the presence of dissipation the system loses such a rigidity, and the scaling behavior turns out to significantly differ. These changes arise from the competition of the rigidity properties of the system at the FOQT and the local dissipation that tends to destroy the nonlocal rigidity. On the other hand, in the case of global dissipators the dynamic scaling resembles that of the single-spin problem. Since they treat globally the system, it is not surprising that the resulting dynamics maintains the main features of the single-spin scenario.

The arguments leading to this scaling scenario at FOQTs are quite general. Analogous phenomena are expected to develop in any homogeneous d-dimensional many-body system at a continuous quantum transition, whose Markovian interactions with the bath can be described by local or extended dissipators within a Lindblad equation (5).

APPENDIX A: THE SINGLE-SPIN MODEL

We consider the following single-spin Hamiltonian:

$$\hat{H}_s = \Delta\,\hat{H}_r\,, \quad \hat{H}_r = \frac{1}{2}\,\hat{\sigma}^{(3)} - \frac{\kappa}{2}\,\hat{\sigma}^{(1)}\,, \tag{A1}$$

where Δ is the energy scale (the gap for $\kappa = 0$), κ is the rescaled parameter related to the intensity of an applied external magnetic field, and $\hat{\sigma}^{(k)}$ are the usual spin-1/2 Pauli matrices. We discuss the dynamics of that single-spin system subject to dissipation, as described by the Lindblad master equation

$$\frac{\partial \rho}{\partial t} = -\frac{i}{\hbar}[\hat{H}_s, \rho] + u\,\mathbb{D}(\rho)\,, \tag{A2}$$

$$\mathbb{D}(\rho) = \hat{L}\rho\hat{L}^\dagger - \tfrac{1}{2}(\rho\,\hat{L}^\dagger\hat{L} + \hat{L}^\dagger\hat{L}\rho)\,. \tag{A3}$$

The protocol starts again from the ground state associated with an initial value κ_i, that is, the pure state

$$|\Psi(t=0)\rangle = \cos(\alpha_i/2)\,|+\rangle + \sin(\alpha_i/2)\,|-\rangle\,, \tag{A4}$$

where $|\pm\rangle$ are the eigenstates of $\hat{\sigma}^{(1)}$ and $\tan(\alpha_i) = \kappa_i^{-1}$. The corresponding density matrix reads

$$\rho(t=0) = \tfrac{1}{2}[\hat{\mathbb{I}} + c_k\hat{\sigma}^{(k)}]\,,$$
$$c_1 = \cos\alpha_i\,, \quad c_2 = 0\,, \quad c_3 = \sin\alpha_i\,, \tag{A5}$$

where $\hat{\mathbb{I}}$ is the 2×2 identity operator. Then the evolution is determined by the Lindblad equation (A2) with coherent driving given by the Hamiltonian at κ (thus for $\kappa \neq \kappa_i$ we have also a quench).

We may generally define the energy of the system as

$$E = \mathrm{Tr}[\rho\hat{H}_s]\,, \tag{A6}$$

whose time derivative allows us to define quantities analogous to the heat q and work w in the time unit, i.e.,

$$\frac{dE}{dt} = \mathrm{Tr}\left[\frac{d\rho}{dt}\hat{H}_s\right] + \mathrm{Tr}\left[\rho\frac{d\hat{H}_s}{dt}\right] \equiv q + w\,. \tag{A7}$$

Using the Lindblad master equation we can easily derive the relation

$$q = \frac{dQ}{dt} = \mathrm{Tr}\left[\frac{d\rho}{dt}\hat{H}_s\right] = u\,\mathrm{Tr}[\mathbb{D}(\rho)\hat{H}_s]\,. \tag{A8}$$

One can easily prove that $q = 0$, if $[\hat{H}, \hat{L}] = 0$.

Moreover we define the *purity*

$$P = \mathrm{Tr}[\rho^2]\,, \tag{A9}$$

which equals one for pure systems. Its time derivative can be written as

$$\frac{dP}{dt} = 2\,\mathrm{Tr}\left[\frac{d\rho}{dt}\rho\right] = 2u\mathrm{Tr}[\mathbb{D}(\rho)\rho]\,. \tag{A10}$$

We may rescale the parameters and the time variable so that

$$\rho'(\theta) \equiv \frac{\partial\rho}{\partial\theta} = -\frac{i}{\hbar}[\hat{H}_r, \rho] + \gamma\,\mathbb{D}(\rho)\,, \tag{A11}$$

$$\theta = t\Delta\,, \quad \gamma = u/\Delta\,. \tag{A12}$$

The time dependent density matrix can be generally parametrized as

$$\rho(\theta) = \frac{1}{2}[\hat{\mathbb{I}} + A_k(\theta)\hat{\sigma}^{(k)}]\,, \quad \sum_k A_k(\theta)^2 \leqslant 1\,, \tag{A13}$$

where A_i are real functions of the rescaled time θ. Note that

$$\mathrm{Tr}[\rho] = 1\,, \quad \mathrm{Tr}[\rho^2] = \frac{1}{2}\left(1 + \sum_k A_k^2\right). \tag{A14}$$

The Lindblad equation (A2) can be turned into coupled differential equations of the functions A_k. Let us consider the Lindblad operators

$$\hat{L}^{\pm} \equiv \hat{\sigma}^{\pm} \equiv \frac{\hat{\sigma}^{(1)} \pm i\hat{\sigma}^{(2)}}{2}\,, \tag{A15}$$

corresponding to the sign + and −, respectively. Straightforward computations lead to the coupled differential equations

$$\begin{aligned} A_1' &= -A_2 - \frac{\gamma}{2}A_1\,,\\ A_2' &= A_1 + \kappa A_3 - \frac{\gamma}{2}A_2\,,\\ A_3' &= -\kappa A_2 - \gamma(A_3 \mp 1)\,. \end{aligned} \tag{A16}$$

The upper/lower signs correspond to the cases $\hat{L}^{\pm}$. The various observables can be written in terms of the function A_i. For example, the longitudinal magnetization M reads

$$\mathcal{M}(\theta) = \mathrm{Tr}[\hat{\sigma}^{(1)}\rho(\theta)] = A_1(\theta)\,. \tag{A17}$$

The heat per unit of rescaled time is given by

$$\begin{aligned} q_r \equiv Q' &= \mathrm{Tr}[\rho'\hat{H}_r] = \frac{1}{2}A_3' - \frac{\kappa}{2}A_1'\\ &= -\frac{\gamma}{2}(A_3 \mp 1) + \frac{1}{4}\gamma\kappa A_1\,. \end{aligned} \tag{A18}$$

The time dependence of the purity (A9) can be easily derived using Eq. (A14) and the above solutions, obtaining

$$P(\theta) = \frac{1}{2}\left(1 + \sum_k A_k(\theta)^2\right) \leqslant 1\,, \tag{A19}$$

$$\begin{aligned} P'(\theta) &= \sum_k A_k(\theta)A_k'(\theta) =\\ &= -\frac{\gamma}{2}\left(A_1^2 + A_2^2\right) - \gamma A_3(A_3 \mp 1)\,. \end{aligned} \tag{A20}$$

In the case $\kappa = 0$, one can easily find the solution

$$\begin{aligned} A_1(\theta) &= e^{-\gamma\theta/2}[A_1(0)\cos(\theta) - A_2(0)\sin(\theta)]\,,\\ A_2(\theta) &= e^{-\gamma\theta/2}[A_1(0)\sin(\theta) + A_2(0)\cos(\theta)]\,,\\ A_3(\theta) \mp 1 &= e^{-\gamma\theta}[A_3(0) \mp 1]\,, \end{aligned} \tag{A21}$$

in terms of the initial density matrix $\rho(0)$ and in particular of its coefficients $A_i(0)$. Therefore we have that

$$q_r = -\frac{\gamma}{2}e^{-\gamma\theta}[A_3(0) \mp 1]\,, \tag{A22}$$

$$Q = \Delta\int_0^{\infty} d\theta\, q_r = -\frac{\Delta}{2}[A_3(0) \mp 1]\,. \tag{A23}$$

Note that Q is positive/negative for pumping/decay (positive Q means that the system is getting energy from the bath). The purity (A9) turns out to exponentially approach one, reflecting the fact the the system relaxes to a pure state.

In the case of *dephasing* Lindblad operator

$$\hat{L}_d \equiv \hat{\sigma}^{(3)}\,, \tag{A24}$$

we obtain the coupled differential equations

$$\begin{aligned} A_1' &= -A_2 - 2\gamma A_1\,,\\ A_2' &= A_1 + \kappa A_3 - 2\gamma A_2\,,\\ A_3' &= -\kappa A_2\,. \end{aligned} \tag{A25}$$

Using the above equations, we derive the heat per unit of rescaled time, which is given by

$$q_r = \mathrm{Tr}[\rho'\hat{H}_r] = \gamma\kappa A_1\,. \tag{A26}$$

Again, for $\kappa = 0$ the solution is quite simple, obtaining

$$\begin{aligned} A_1(\theta) &= e^{-2\gamma\theta}[A_1(0)\cos(\theta) - A_2(0)\sin(\theta)]\,,\\ A_2(\theta) &= e^{-2\gamma\theta}[A_1(0)\sin(\theta) + A_2(0)\cos(\theta)]\,,\\ A_3(\theta) &= A_3(0)\,. \end{aligned} \tag{A27}$$

No heat transmission occurs, because $[\hat{H}, \hat{L}] = 0$ when $\kappa = 0$. On the other hand the purity changes

$$P(\theta) = \tfrac{1}{2}\{1 + A_3(0)^2 + e^{-4\gamma\theta}[A_1(0)^2 + A_2(0)^2]\}\,, \tag{A28}$$

approaching exponentially the asymptotic value

$$P(\theta \to \infty) = \frac{1 + A_3(0)^2}{2}\,. \tag{A29}$$

Therefore, the spin system relaxes to a mixed state under dephasing.

APPENDIX B: QUANTUM THERMODYNAMICS OF A FERMIONIC WIRE COUPLED TO LOCAL BATHS

In this Appendix we focus on the quantum thermodynamics of fermionic quantum wires coupled to local Markovian baths. In particular, we consider a Kitaev quantum wire defined by the Hamiltonian [39]

$$\hat{H}_K = -J \sum_{x=1}^{L} \left(\hat{c}_x^\dagger \hat{c}_{x+1} + \delta\, \hat{c}_x^\dagger \hat{c}_{x+1}^\dagger + \text{H.c.} \right) - \mu \sum_{x=1}^{L} \hat{n}_x \,, \quad \text{(B1)}$$

where $\hat{c}_x$ is the fermionic annihilation operator associated with the sites of the chain of size L, $\hat{n}_x \equiv \hat{c}_x^\dagger \hat{c}_x$ is the density operator, and $\delta > 0$. We set $\hbar = 1$, and $J = 1$ as the energy scale. We consider antiperiodic boundary conditions, $\hat{c}_{L+1} = -\hat{c}_1$, and even L for computational convenience.

The Hamiltonian (B1) can be mapped into a spin-1/2 XY chain, through a Jordan-Wigner transformation [5]. In the following we fix $\delta = 1$ (without loss of generality), so that the corresponding spin model is the quantum Ising chain (1). Note however that the nonlocal Jordan-Wigner transformation of the Ising chain with periodic or antiperiodic boundary conditions does not map into the fermionic model (B1) with periodic or antiperiodic boundary conditions. Indeed further considerations apply [24,40], leading to a less straightforward correspondence, depending on the parity of the particle number eigenvalue. Therefore, the Kitaev quantum wire cannot be considered completely equivalent to the quantum Ising chain (see, e.g., the discussion in the Appendix of Ref. [10]). However, analogously to the quantum Ising chain, the Kitaev quantum wire undergoes a continuous quantum transition at $\mu = \mu_c = -2$, between a disordered ($\mu < \mu_c$) and an ordered quantum phase ($|\mu| < |\mu_c|$). This transition belongs to the two-dimensional Ising universality class [5], characterized by the length-scale critical exponent $\nu = 1$, related to the renormalization-group dimension $y_\mu = 1/\nu = 1$ of the Hamiltonian parameter μ (more precisely of the difference $\bar{\mu} \equiv \mu - \mu_c$). The dynamic exponent associated with the unitary quantum dynamics is $z = 1$.

We focus on the out-of-equilibrium thermodynamic behavior of the Fermi lattice gas close to its continuous quantum transition in the presence of homogeneous dissipation mechanisms described by the Lindblad equation (5). We consider local dissipative mechanisms, so that $\mathbb{D}[\rho] = \sum_x \mathbb{D}_x[\rho]$ is given by a sum of local (single-site) terms (top drawing of Fig. 1). The onsite Lindblad operators $\hat{L}_x$ describe the coupling of each site with an independent bath $\mathcal{B}$, associated with particle loss (l) or pumping (p), thus

$$\hat{L}_{\text{l},x} = \hat{c}_x, \quad \hat{L}_{\text{p},x} = \hat{c}_x^\dagger \,, \quad \text{(B2)}$$

respectively. With this choice of dissipators, the full open-system many-body fermionic master equation enjoys a particularly simple treatment.

As a matter of fact, we mention that the out-of-equilibrium dynamics of the Kitaev quantum chain with such kind of dissipators has been the object of several studies in different contexts (see, e.g., Refs. [41–44]). One of them concerns the behavior of the fermionic correlation functions resulting from a sudden quench [8,9]. Namely, one considers a protocol that starts from the ground state $|0_{\mu_i}\rangle$ of $\hat{H}_K$ for a generic μ_i. The system is then let free to evolve after a quench of the Hamiltonian parameter to μ, at $t = 0$ and a simultaneous turning on of the interaction with the environment controlled by the dissipation coupling u. Below we discuss further aspects of such dynamics, which have not been considered so far.

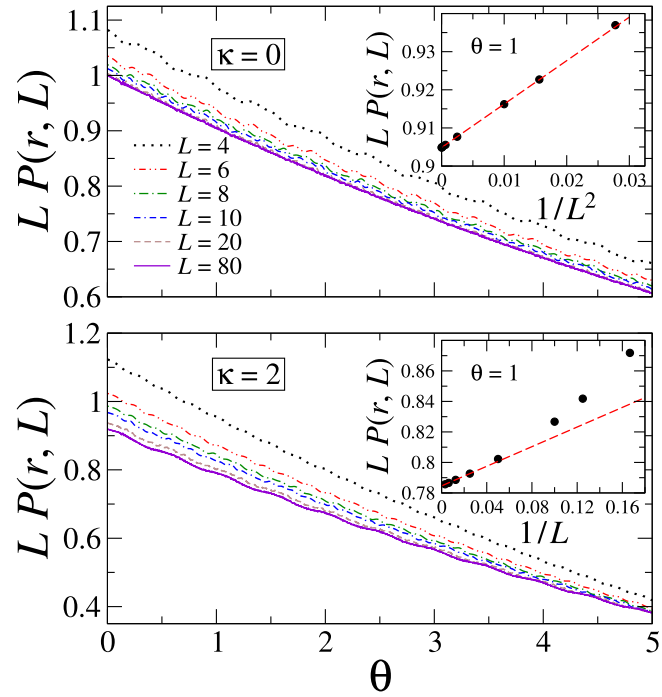

FIG. 7. Time behavior of the correlation function $P(r,t)$ for the Kitaev quantum wire close to the CQT point ($\delta = 1$, $\mu = -2$). The system is driven out of equilibrium by the coupling with an external bath in the Lindblad form, under the form of local and uniform incoherent particle losses with rescaled strength $\gamma = 0.1$. The top figure shows data for $\kappa_i = \kappa = 0$ (i.e., the Hamiltonian is exactly at the CQT), while the bottom figure is for $\kappa_i = \kappa = 2$. The various curves in the two main panels show $L\,P(r,t)$ for $r = L/2$ and different chain lengths L (see legend), as a function of the rescaled time θ. In the insets we report the same quantity as a function of L^{-2} (top) or of L^{-1} (bottom), for a fixed value of $\theta = 1$. To perform this analysis, we have first washed out the wiggles in θ (see main plot), by fitting the original curves in the interval $\theta \in [0, 5]$ with a fifth-order polynomial.

Before presenting the analysis of the quantum thermodynamic properties during the time evolution associated with the above protocol, let us come back to the following correlation function at distance r:

$$P(r,t) = \text{Tr}[\rho(t)\,(\hat{c}_x^\dagger \hat{c}_{x+r}^\dagger + \hat{c}_{x+r}\hat{c}_x)] \,. \quad \text{(B3)}$$

This is expected to converge, in the large-L limit, to the asymptotic dynamic scaling behavior [8]

$$P(r,t,\bar{\mu}_i,\bar{\mu}_f,u,L) \approx L^{-1}\mathcal{P}(R,\theta,\kappa_i,\kappa,\gamma) \,, \quad \text{(B4)}$$

where $R = r/L$ and the other scaling variables are defined as usual. The data reported in Fig. 7 display the approach to such scaling behavior, after keeping the scaling variables

fixed, where

$$\theta = tL^{-z}, \quad \gamma = uL^{z}, \quad \kappa(\mu) = \bar{\mu}L^{y_\mu},$$
$$\bar{\mu} = \mu - \mu_c, \quad \kappa_i \equiv \kappa(\mu_i), \quad \kappa \equiv \kappa(\mu). \tag{B5}$$

The large-L asymptotic behavior turns out to be approached with power-law suppressed corrections, analogously to what has been hinted in the main text for the dissipative quantum Ising chain. The approach to the asymptotic behavior is generally characterized by $O(1/L)$ corrections, except at the critical point where they may get suppressed by a larger $O(1/L^2)$ power [9,10,37], as also shown by the insets of Fig. 7. Further results for the asymptotic large-L behavior of the fermionic correlations functions can be found in Refs. [8,9].

We now extend the analysis of the out-of-equilibrium dynamics arising from the protocol described above to the quantum thermodynamics, focussing on the quantum work and heat interchange during the out-of-equilibrium evolution. We discuss the case of particle decay as a dissipative mechanism; the case of pumping can be easily obtained by analogous computations.

The first law of thermodynamics (11) describes the energy flows of the global system, including the environment. In our protocol, a nonvanishing work is only done at $t = 0$, if the Hamiltonian parameter μ is suddenly changed from μ_i to $\mu \neq \mu_i$. Since after quenching the Hamiltonian is kept fixed, thus $w(t) = 0$ for $t > 0$, and the average work is just given by

$$W = \langle 0_{\mu_i}|\hat{H}_K(\mu) - \hat{H}_K(\mu_i)|0_{\mu_i}\rangle$$
$$= (\mu_i - \mu)L\,\langle 0_{\mu_i}|\hat{n}_x|0_{\mu_i}\rangle, \tag{B6}$$

where the last expression is obtained because the antiperiodic boundary conditions respect translational invariance. The matrix element of the particle density $\hat{n}_x$ can be computed analytically, in particular when $\mu_i = \mu_c$, we have

$$\langle 0_{\mu_c}|\hat{n}_x|0_{\mu_c}\rangle = D(L), \tag{B7}$$

$$D(L) = \frac{1}{2} - \frac{\sin\left(\frac{\pi}{2L}\right)}{L\left[1-\cos\left(\frac{\pi}{L}\right)\right]} = \frac{\pi-2}{2\pi} + \frac{\pi}{24L^2} + O(L^{-4}). \tag{B8}$$

More generally, for μ in the critical region, so that $\bar{\mu} \equiv \mu - \mu_c \ll 1$, we obtain the asymptotic expansion [37]

$$\langle 0_\mu|\hat{n}_x|0_\mu\rangle = f_a(\bar{\mu}) + L^{-\zeta} f_s(\kappa) + O(L^{-2}), \tag{B9}$$

where $\zeta = 1 + z - y_\mu = 1$, f_a and f_s are appropriate functions.

Concerning the heat interchanged with the environment, we derive the nontrivial relation

$$q(t) = -u\,\mathrm{Tr}[\rho(t)\hat{H}_K(\mu)], \tag{B10}$$

obtained by replacing $\partial_t \rho(t)$ using the Lindblad equation for the density matrix and further manipulations related to the particular structure of the Lindblad dissipator $\mathbb{D}_j[\rho]$. Moreover, since the Hamiltonian is independent of the time for $t > 0$, we also have

$$q(t) = \mathrm{Tr}\left[\frac{d\rho(t)}{dt}\hat{H}_K(\mu)\right] = \frac{d}{dt}\mathrm{Tr}\left[\rho(t)\hat{H}_K(\mu)\right] = \frac{dE_s}{dt}. \tag{B11}$$

Then using Eqs. (B10) and (B11), we obtain

$$q(t) = -u\,\mathrm{Tr}\left[\rho(0)\hat{H}_K(\mu)\right] e^{-ut}$$
$$= -u\,\langle 0_{\mu_i}|\hat{H}_K(\mu)|0_{\mu_i}\rangle\, e^{-ut}. \tag{B12}$$

Note that

$$\langle 0_{\mu_i}|\hat{H}_K(\mu)|0_{\mu_i}\rangle = E_{0_{\mu_i}} + W, \tag{B13}$$

where $E_{0_{\mu_i}} = \langle 0_{\mu_i}|\hat{H}_K(\mu_i)|0_{\mu_i}\rangle$ is the ground-state energy at μ_i, and W is the average work done at $t = 0$, cf. Eq. (B6). In particular for $\bar{\mu}_i = 0$

$$\langle 0_{\mu_c}|\hat{H}_K(\mu)|0_{\mu_c}\rangle = L\,[4D(L) - 1 + \bar{\mu}D(L)]$$
$$= L\left[\frac{\pi-4}{\pi} - \bar{\mu}\frac{\pi-2}{2\pi} + O(L^{-2})\right]. \tag{B14}$$

Equilibrium computations around the critical point give the general structure [37]

$$\langle 0_{\mu_i}|\hat{H}_K(\mu)|0_{\mu_i}\rangle = Lg_a(\bar{\mu}_i, \bar{\mu}) + L^{-1}g_s(\kappa_i, \kappa) + O(L^{-2}). \tag{B15}$$

Finally, we obtain

$$Q(t) = \int_0^t dt\, q(t) = \langle 0_{\mu_i}|\hat{H}_K(\mu)|0_{\mu_i}\rangle(e^{-ut} - 1). \tag{B16}$$

The above results have also been carefully checked numerically, since very accurate results for large lattice sizes [$L = O(10^3)$] can be easily obtained exploiting the particular structure of the Lindblad equations for the system considered [8,9].

Let us finally address the scaling behavior at the critical point of the above results. In particular, we note that the average work asymptotically behaves as

$$W = L\,\bar{\mu}_i\, f_a(\bar{\mu}_i) + L^{-1}(\kappa_i - \kappa)f_s(\kappa_i) + O(L^{-2}). \tag{B17}$$

Its structure does not apparently agree with the general scaling behaviors put forward in Ref. [35]. Indeed, taking into account that $y_n = 1$ is the renormalization-group dimension of the perturbation involved by the quench of the parameter μ, which is the density operator $\hat{n}_x$, one would expect

$$W \approx L^{-z}F_s(\kappa_i, \kappa), \tag{B18}$$

with $z = 1$, which matches the subleading term in the expansion (B17). Equation (B18) is supposed to be the asymptotic behavior keeping κ_i and κ fixed. This apparent contradiction is explained by contributions arising from short-ranged fluctuations like those giving rise to the analytic part of the free energy at the critical point [37]. In other words, this is related to the mixing of the perturbation considered, i.e., the particle density operator $\sum_x \hat{n}_x$, with the identity operator, which leads to the leading term in Eq. (B9). On the other hand, Ref. [35] considered perturbations not showing such problems, such as the longitudinal spin operator in the quantum Ising chain. Generally, quenches associated with perturbations vanishing at the critical point, by symmetry, give rise to an average works satisfying the scaling laws reported in Ref. [35].

Analogous considerations apply to the behavior of the heat interchange around the critical point. Indeed, using Eq. (B15), we may rewrite the expression of q, cf. Eq. (B12), in terms of

dynamic scaling variables (B5), obtaining

$$q(t) \approx L\, G_a(t, \mu_i, \mu, u) + L^{-2} G_s(\theta, \kappa_i, \kappa, \gamma)\,, \qquad \text{(B19)}$$

where the scaling part is again the subleading term associated with the scaling function

$$G_s(\theta, \kappa_i, \kappa, \gamma) = -\gamma e^{-\gamma\theta} g_s(\kappa_i, \kappa)\,. \qquad \text{(B20)}$$

However, we should observe that disentangling the $O(L^{-2})$ scaling part from the leading $O(L)$ term turns out to be a very hard task in practice, due also to the fact that the different variables of the two terms, with their different L dependence, makes such distinction of doubtful value. Therefore, we do not pursue this issue further.

[1] A. A. Houck, H. E. Türeci, and J. Koch, On-chip quantum simulation with superconducting circuits, Nat. Phys. **8**, 292 (2012).

[2] M. Müller, S. Diehl, G. Pupillo, and P. Zoller, Engineered open systems and quantum simulations with atoms and ions, Adv. At. Mol. Opt. Phys. **61**, 1 (2012).

[3] I. Carusotto and C. Ciuti, Quantum fluids of light, Rev. Mod. Phys. **85**, 299 (2013).

[4] M. Aspelmeyer, T. J. Kippenberg, and F. Marquardt, Cavity optomechanics, Rev. Mod. Phys. **86**, 1391 (2014).

[5] S. Sachdev, *Quantum Phase Transitions* (Cambridge University Press, Cambridge, 1999).

[6] S. Yin, P. Mai, and F. Zhong, Nonequilibrium quantum criticality in open systems: The dissipation rate as an additional indispensable scaling variable, Phys. Rev. B **89**, 094108 (2014).

[7] S. Yin, C.-Y. Lo, and P. Chen, Scaling behavior of quantum critical relaxation dynamics of a system in a heat bath, Phys. Rev. B **93**, 184301 (2016).

[8] D. Nigro, D. Rossini, and E. Vicari, Competing coherent and dissipative dynamics close to quantum criticality, Phys. Rev. A **100**, 052108 (2019).

[9] D. Rossini and E. Vicari, Scaling behavior of the stationary states arising from dissipation at continuous quantum transitions, Phys. Rev. B **100**, 174303 (2019).

[10] D. Rossini and E. Vicari, Dynamic Kibble-Zurek scaling framework for open dissipative many-body systems crossing quantum transitions, Phys. Rev. Research **2**, 023211 (2020).

[11] M. Campostrini, J. Nespolo, A. Pelissetto, and E. Vicari, Finite-Size Scaling at First-Order Quantum Transitions, Phys. Rev. Lett. **113**, 070402 (2014).

[12] A. Pelissetto, D. Rossini, and E. Vicari, Finite-size scaling at first-order quantum transitions when boundary conditions favor one of the two phases, Phys. Rev. E **98**, 032124 (2018).

[13] A. Pelissetto, D. Rossini, and E. Vicari, Scaling properties of the dynamics at first-order quantum transitions when boundary conditions favor one of the two phases, Phys. Rev. E **102**, 012143 (2020).

[14] V. Piazza, V. Pellegrini, F. Beltram, W. Wegscheider, T. Jungwirth, and A. H. MacDonald, First-order phase transitions in a quantum Hall ferromagnet, Nature (London) **402**, 638 (1999).

[15] T. Vojta, D. Belitz, T. R. Kirkpatrick, and R. Narayanan, Quantum critical behavior of itinerant ferromagnets, Ann. Phys. (Leipzig) **8**, 593 (1999).

[16] M. Uhlarz, C. Pfleiderer, and S. M. Hayden, Quantum Phase Transitions in the Itinerant Ferromagnet $ZrZn_2$, Phys. Rev. Lett. **93**, 256404 (2004).

[17] C. Pfleiderer, Why first order quantum phase transitions are interesting, J. Phys.: Condens. Matter **17**, S987 (2005).

[18] W. Knafo, S. Raymond, P. Lejay, and J. Flouquet, Antiferromagnetic criticality at a heavy-fermion quantum phase transition, Nat. Phys. **5**, 753 (2009).

[19] T. Jörg, F. Krzakala, J. Kurchan, and A. C. Maggs, Simple Glass Models and Their Quantum Annealing, Phys. Rev. Lett. **101**, 147204 (2008).

[20] T. Jörg, F. Krzakala, G. Semerjian, and F. Zamponi, First-Order Transitions and the Performance of Quantum Algorithms in Random Optimization Problems, Phys. Rev. Lett. **104**, 207206 (2010).

[21] A. P. Young, S. Knysh, and V. N. Smelyanskiy, First Order Phase Transition in the Quantum Adiabatic Algorithm, Phys. Rev. Lett. **104**, 020502 (2010).

[22] Y. Seki and H. Nishimori, Quantum annealing with antiferromagnetic fluctuations, Phys. Rev. E **85**, 051112 (2012).

[23] A. Nava and M. Fabrizio, Lindblad dissipative dynamics in the presence of phase coexistence, Phys. Rev. B **100**, 125102 (2019).

[24] P. Pfeuty, The one-dimensional Ising model with a transverse field, Ann. Phys. **57**, 79 (1970).

[25] V. Privman and M. E. Fisher, Finite-size effects at first-order transitions, J. Stat. Phys. **33**, 385 (1983).

[26] G. G. Cabrera and R. Jullien, Role of boundary conditions in the finite-size Ising model, Phys. Rev. B **35**, 7062 (1987).

[27] H.-P. Breuer and F. Petruccione, *The Theory of Open Quantum Systems* (Oxford University Press, New York, 2002).

[28] A. Rivas and S. F. Huelga, *Open Quantum Systems: An Introduction* (Springer, New York, 2012).

[29] L. M. Sieberer, M. Buchhold, and S. Diehl, Keldysh field theory for driven open quantum systems, Rep. Prog. Phys. **79**, 096001 (2016).

[30] G. Lindblad, On the generators of quantum dynamical semigroups, Commun. Math. Phys. **48**, 119 (1976).

[31] V. Gorini, A. Kossakowski, and E. C. G. Sudarshan, Completely positive dynamical semigroups of N-level systems, J. Math. Phys. **17**, 821 (1976).

[32] S. Deffner and S. Campbell, *Quantum Thermodynamics: An Introduction to the Thermodynamics of Quantum Information* (Morgan and Claypool, San Rafael, 2019).

[33] F. Binder, L. A. Correa, C. Gogolin, J. Anders, and G. Adesso, *Thermodynamics in the Quantum Regime. Fundamental Theories of Physics* (Springer International Publishing, Cham, 2018).

[34] J. Gemmer, M. Michel, and G. Mahler, *Quantum Thermodynamics: Emergence of Thermodynamic Behavior Within Composite Quantum Systems* (Springer-Verlag, Berlin, 2004).

[35] D. Nigro, D. Rossini, and E. Vicari, Scaling properties of work fluctuations after quenches near quantum transitions, J. Stat. Mech. (2019) 023104.

[36] D. Rossini and E. Vicari, Scaling of decoherence and energy flow in interacting quantum spin systems, Phys. Rev. A **99**, 052113 (2019).

[37] M. Campostrini, A. Pelissetto, and E. Vicari, Finite-size scaling at quantum transitions, Phys. Rev. B **89**, 094516 (2014).

[38] A. Pelissetto, D. Rossini, and E. Vicari, Dynamic finite-size scaling after a quench at quantum transitions, Phys. Rev. E **97**, 052148 (2018).

[39] A. Yu. Kitaev, Unpaired Majorana fermions in quantum wires, Phys. Usp. **44**, 131 (2001).

[40] S. Katsura, Statistical mechanics of the anisotropic linear Heisenberg model, Phys. Rev. **127**, 1508 (1962).

[41] T. Prosen, Third quantization: A general method to solve master equations for quadratic open Fermi systems, New J. Phys. **10**, 043026 (2008).

[42] B. Horstmann, J. I. Cirac, and G. Giedke, Noise-driven dynamics and phase transitions in fermionic systems, Phys. Rev. A **87**, 012108 (2013).

[43] M. Keck, S. Montangero, G. E. Santoro, R. Fazio, and D. Rossini, Dissipation in adiabatic quantum computers: Lessons from an exactly solvable model, New J. Phys. **19**, 113029 (2017).

[44] S. Bandyopadhyay, S. Bhattacharjee, and A. Dutta, Dynamical generation of Majorana edge correlations in a ramped Kitaev chain coupled to nonthermal dissipative channels, Phys. Rev. B **101**, 104307 (2020).